THE BELL SYSTEM TECHNICAL JOURNAL
Vol. 53, No. 7, September 1974
Printed in U.S.A.

Application of Response-Bound Method in Shock and Vibration Analysis of Telephone Structures

By S. C. LIU

(Manuscript received December 10, 1973)

Telephone structures must remain in operation during the shock and vibration caused by blasts, earthquakes, or other dynamic forces. Traditionally, various numerical methods, including the finite element approach, have been used to analyze such problems. These methods, although effective, generally require excessive and costly computations. In contrast, the Fourier transform method used in conjunction with a fast Fourier transform algorithm is much more economical. In addition, shock and vibration problems involving frequency-dependent parameters can be effectively treated by the Fourier method. However, to make the Fourier method more effective and widely applicable, various tractable input-transfer-output relations are needed. This paper derives a set of simple equality and inequality relations that allow various response parameters to be conveniently estimated based on partial knowledge of the input and the structures. In particular, two lower bounds and eight upper bounds of the maximum response of linear structures are presented. Simple structures subjected to impulse loads resembling blasts and a random transient load resembling earthquakes are studied. Practical applications of the method to telephone structures are demonstrated by the analysis of a battery stand and a community dial office system in an earthquake area.

I. INTRODUCTION

The Fourier transform method has long been used to characterize linear systems and to identify the frequency content of waveforms. Sneddon[1] demonstrates classical applications of the Fourier transform method to engineering and physics problems. Amba-Rao[2] gives recent applications of this method to elasticity, White[3] illustrates system response calculations, Le Bail[4] demonstrates boundary-value problems

in physics, and Liu and Fagel[5,6] analyze earthquake soil-structure interactions. In the last three applications cited, the fast Fourier transform (FFT) algorithms were used in conjunction with the Fourier method to obtain numerical solutions. The development of FFT algorithms in the past few years has rapidly expanded the application of the Fourier method to include digital analysis of linear-system dynamics.

This work was motivated by the idea that some simple and effective techniques based on the Fourier transform method and response-bound relations of linear systems can be developed for the shock and vibration analysis of telephone structures.

This paper discusses the Fourier transform method applied to the vibration problems of linear structures and presents some simple relationships that make it possible to quickly evaluate and estimate various response parameters. In a typical engineering vibration problem, the primary concerns are the time and frequency aspects of the input and output (response) and the transfer characteristics of the system or structure involved. The parameters or functions of interest are generally the waveforms of input and output, their Fourier transforms, the peak values, the frequency characteristics of these waveforms, and the effects of linear filtering by structures. Of further concern are the time and frequency distributions of energy or power of these waveforms and, particularly, the analytical and empirical relations among all the parameters and functions mentioned above. In view of the advance of computational techniques, some well-known and lesser-known input-transfer-output relations useful to shock and vibration analysis should be systematically presented. The purpose of this paper is to make these relations available, to discuss their implications, and to demonstrate their applications.

II. BACKGROUND AND THEORETICAL BASIS

Applied to the engineering vibration problem, the basic concept of the Fourier method of analysis is very simple. We assume that the structure under consideration is linear, causal, and stable, and its property is completely defined by the associated transfer function pairs $h(t) \leftrightarrow H(i\omega)$, where $H(i\omega)$ is the frequency response function, $h(t)$ is the impulse response function, t is the time variable, ω is the frequency variable, i is the complex unit, and the symbol $\leftrightarrow$ indicates a Fourier transform (FT) pair. When the structure is excited by an arbitrary (deterministic or random) input function, $x(t) \leftrightarrow X(i\omega)$, the response is given as $y(t) \leftrightarrow Y(i\omega)$. If $X(i\omega)$ and $H(i\omega)$ are known, the response can be obtained by using the simple relationship, $y(t)$

$= x(t)*h(t)$, where $*$ indicates convolution, or by using $Y(i\omega) = X(i\omega)H(i\omega)$ and taking the inverse FT of $Y(i\omega)$. Other response quantities of interest can also be obtained from the basic FT pairs $x(t) \leftrightarrow X(i\omega)$, $h(t) \leftrightarrow H(i\omega)$, and $y(t) \leftrightarrow Y(i\omega)$ once their relations and the pertinent response parameter are found. This approach is efficient because no numerical integrations are required (as in many traditional methods of analysis), and it yields all needed solutions in both the time and frequency domains with simple discrete FT or FFT computer routines now generally available. However, the Fourier method of analysis is particularly attractive and powerful because of the availability of some analytical input-transfer-output relations as described in this paper. These relations, in the form of simple equality or inequality, can solve many practical problems. Some important preliminary background material, particularly the definition and properties of an arbitrary shock function, $f(t)$, will be briefly given before the main results.

2.1 Shock function and related quantities

A time function $f(t)$, $t \in [a, b]$ for finite $a > b \geqq 0$ is referred to as a shock function. Without losing generality, it is assumed that $f(t)$ begins at $t = 0$ and has finite duration T, i.e., $a = 0$ and $b = T$. The shock function $f(t)$ could be the input $x(t)$, the output $y(t)$, or the impulse response function of the system $h(t)$, and it could be either deterministic or random. Associated with a shock function $f(t)$, the following quantities of interest are defined:

Fourier Transform:

$$F(i\omega) = \int_0^T f(t) \exp(-i\omega t)dt. \tag{1a}$$

Running FT or Spectrum:

$$F(t, i\omega) = \int_0^t f(\tau) \exp(-i\omega\tau)d\tau. \tag{1b}$$

Energy:

$$E_f(t) = \int_0^t f^2(\tau)d\tau = \frac{1}{2\pi}\int_{-\infty}^{\infty} |F(t, i\omega)|^2 d\omega. \tag{1c}$$

Total Energy:

$$E_f = \int_0^T f^2(t)dt = \frac{1}{2\pi}\int_{-\infty}^{\infty} |F(i\omega)|^2 d\omega. \tag{1d}$$

Instantaneous Power Spectrum:

$$\rho_f(t, i\omega) = \frac{\partial}{\partial t} |F(t, i\omega)|^2. \tag{1e}$$

Power:

$$P_f(t) = \frac{dE_f(t)}{dt} = \frac{1}{2\pi} \int_{-\infty}^{\infty} \rho_f(t, i\omega) d\omega. \tag{1f}$$

Frequency Moment:

$$M_{f,n} = \frac{1}{2\pi} \int_{-\infty}^{\infty} |\omega|^n |F(i\omega)| d\omega \quad n = 0, 1, 2, \cdots. \tag{1g}$$

Time Moment:

$$m_{f,n} = \int_0^T |t|^n |f(t)| dt \quad n = 0, 1, 2, \cdots. \tag{1h}$$

Frequency Variation:

$$S_{f,n} = \frac{1}{2\pi} \int_{-\infty}^{\infty} |F^{(n)}(i\omega)| d\omega, \quad n = 0, 1, 2, \cdots. \tag{1i}$$

Time Variation:

$$s_{f,n} = \int_0^T |f^{(n)}(t)| dt, \quad n = 0, 1, 2, \cdots. \tag{1j}$$

Correlation Function:

$$R_f(\tau) = f(t)*f(t) = \int_0^T f(t)f(t - \tau)dt. \tag{1k}$$

Note that some of these quantities, e.g., $M_{f,n}$ and $m_{f,n}$, may not exist. Some simple bounds on $f(t)$, $F(\omega)$, and their derivatives, which will be used to derive response relations, can be readily obtained from the above equations.

2.2 Some bounds of shock function and related quantities

2.2.1 Derivative bounds

The following inequalities relating the derivatives of a shock function or of its FT with various signal parameters can be established.

$$|f^{(n)}(t)| \leqq M_n \qquad n = 0, 1, 2, \cdots. \tag{2a}$$

$$|f^{(n)}(t)| \leqq \Omega^n \left[\frac{E_f \Omega}{(2n + 1)\pi} \right]^{\frac{1}{2}} \quad n = 0, 1, 2, \cdots. \tag{2b}$$

$$|F^{(n)}(i\omega)| \leqq m_n \qquad n = 0, 1, 2, \cdots. \tag{2c}$$

$$|F^{(n)}(i\omega)| \leqq T^n \left(\frac{E_f T}{2n + 1} \right)^{\frac{1}{2}} \quad n = 0, 1, 2, \cdots. \tag{2d}$$

These relations can be proved as follows. The nth derivatives $f^{(n)}(t) = d^n f(t)/dt^n$ and $F^n(i\omega) = d^n F(i\omega)/d\omega^n$ $(n = 0, 1, 2, \cdots)$, can be written as

$$f^{(n)}(t) = \frac{1}{2\pi} \int_{-\infty}^{\infty} (i\omega)^n F(i\omega) \exp(i\omega t) d\omega \tag{3a}$$

and

$$F^{(n)}(i\omega) = \int_0^T (-it)^n f(t) \exp(-i\omega t) dt. \tag{3b}$$

Equations (2a) follows from (3a) and (1g), and (2c) follows from (3b) and (1h). Note that (2a) and (2c) are analogous bounds in terms of frequency and time moments, respectively. Equations (2b) and (2d) follow from (3a) and (3b), respectively, and Schwartz inequality. In (2b), Ω is a constant and is defined as $F(i\omega) \cong 0$ for $|\omega| \geqq \Omega$; i.e., in the practical sense, the shock function $f(t)$ is assumed to be essentially band-limited. Although a shock function cannot be strictly band-limited, in practice most functions (except ideal impulses) possess a frequency value beyond which the Fourier spectra are negligibly small. Furthermore, because the sample rate can never be infinitely large, digitization of the time function always imposes a practical band-limit. Although the details are beyond the scope of this paper, various methods and criteria are available for the construction of equivalent band-limited signals. Equations (2b) and (2d) are also analogous bounds in terms of energy.

2.2.2 Amplitude bounds

$$|f(t)| \leqq \left(\frac{E_f \Omega}{\pi}\right)^{\frac{1}{2}}, \quad \text{for all } t, \tag{4a}$$

$$|F(i\omega)| \leqq (E_f T)^{\frac{1}{2}}, \quad \text{for all } \omega, \tag{4b}$$

$$|f(t)| \leqq \frac{S_{f,n}}{t^n}, \quad \text{for all } t, \quad n = 0, 1, 2, \cdots, \tag{4c}$$

$$|F(i\omega)| \leqq \frac{S_{f,n}}{|\omega|^n}, \quad \text{for all } \omega, \quad n = 0, 1, 2, \cdots. \tag{4d}$$

When $n = 0$, (4a) and (4b) are special cases of (2b) and (2d), respectively. From the relation $(-it)^n f(t) \leftrightarrow F^{(n)}(i\omega)$, the following relation holds:

$$|f(t)| \leqq |(it)^{-n}| \frac{1}{2\pi} \int_{-\infty}^{\infty} |F^{(n)}(i\omega)| d\omega. \tag{5}$$

Relation (4c) is obtained from (1i) and (5). Note that in (4c) no

band-limitedness requirement is needed. Similarly, the relation $f^{(n)}(t) \leftrightarrow (i\omega)^n F(i\omega)$, eq. (1j), and

$$|F(i\omega)| \leqq |(i\omega)^{-n}| \int_{-\infty}^{\infty} |f^{(n)}(t)|\, dt \tag{6}$$

lead to (4d). When (4c) [or (4d)] is used, better bounds are provided for small t (or ω) when n is small, and for large t (or ω) when n is large.

2.2.3 Increment bounds

Let $\delta_f = f(t + \Delta t) - f(t)$ and $\delta_F = F[i(\omega + \Delta\omega)] - F(i\omega)$, then

$$|\delta_f| \leqq M_1 \Delta t, \tag{7a}$$

$$|\delta_f| \leqq \left[\frac{2E_f\Omega}{\pi}\left(1 - \frac{\sin \Omega\Delta t}{\Omega\Delta t}\right)\right]^{\frac{1}{2}} \leqq \Omega\Delta t\left(\frac{E_f\Omega}{3\pi}\right), \tag{7b}$$

$$|\delta_F| \leqq m_1 \Delta\omega, \tag{7c}$$

and

$$|\delta_F| \leqq \left[2E_f T\left(1 - \frac{\sin T\Delta\omega}{T\Delta\omega}\right)\right]^{\frac{1}{2}} \leqq T\Delta\omega\left(\frac{E_f T}{3}\right)^{\frac{1}{2}}. \tag{7d}$$

Relations (7a) and (7c) are special cases (when $n = 1$) of (2a) and (2c), respectively. Equations (7b) and (7d) follow from (1a) and the corresponding inverse FT relation, respectively, and from Schwartz inequality. Note that the band-limitedness requirement is imposed to derive (7b). Equations (7a) and (7c) are analogous increment bounds in terms of moments; (7b) and (7d) are analogous bounds in terms of energy. Kak[7] proves (2d), (4b), and (7d), while Papoulis[8,9] proves (2b), (4a), and (7b).

The equality conditions for the above relations can be easily identified. For example, the equality holds for (2d) when $f(t) = C(it)^n$ for even n and a constant C, for (4b) when $f(t) = C \exp(i\omega_o t)$, when $\omega_o = n\pi/T$, and $n = 0, 1, 2, \cdots$, and for (7d) when $f(t) = 2(1 - \sin \Delta\omega)^{\frac{1}{2}}$. Analogous conditions apply to their analogous counterrelations and can be established straightforwardly.

2.2.4 Energy bounds

Let $f_m = \max |f(t)|$, occurring at $t = t_f$, and $F_m = \max |F(i\omega)|$, occurring at $\omega = \omega_F$. Then

$$F_m^2 T^{-1} \leqq E_f \leqq f_m^2 T \quad \text{for all } \omega. \tag{8}$$

The upper bound is obvious from the definition of E_f given in (1d); the lower bound follows from applying Schwartz inequality to the

relation

$$F(i\omega) = \int_0^T f(t) \exp(-i\omega t)dt,$$

which results in

$$|F(i\omega)|^2 \leqq \int_0^T |f(t)|^2 dt \int_0^T |\exp(-i\omega t)|^2 dt \leqq E_f T \quad \text{for all } \omega. \quad (9)$$

III. RELATIONS FOR VARIOUS RESPONSE PARAMETERS

The basic properties of a general shock function and its FT provide the basis for establishing important equality and inequality relations for various response parameters of linear systems. Let $x(t) \leftrightarrow X(i\omega)$, $h(t) \leftrightarrow H(i\omega)$, and $y(t) \leftrightarrow Y(i\omega)$ represent, respectively, the FT pair of the input, the transfer function, and the response; $x(t)$, $h(t)$, and $y(t)$ are shock functions; therefore, the basic definitions and properties are applicable. The functions $x(t)$, $h(t)$, and $y(t)$ are assumed to possess time duration T_x, T_h, and T_y and are band-limited within ω_X, ω_H, and ω_Y. It is obvious that $T_y = T_x + T_y$, and $\Omega_Y = \min(\Omega_X, \Omega_H)$. Let $x_m = \max|x(t)|$, $h_m = \max|h(t)|$, $y_m = \max|y(t)|$, $X_m = \max|X(i\omega)|$, $H_m = \max|H(i\omega)|$, and $Y_m = \max|Y(i\omega)|$, and t_x, t_h, t_y, ω_X, ω_H, and ω_Y be the corresponding times and frequencies these maxima occur. Note that t_x, t_h, and t_y or ω_X, ω_H, and ω_Y need not be equal. In addition to the well-known basic input-transfer-output relationships $y(t) = x(t)*h(t)$ and $Y(i\omega) = X(i\omega)H(i\omega)$, the important relations that follow can be established.

3.1 Total energy bounds

The total energy of $x(t)$, $h(t)$, or $y(t)$ is bounded by the peak amplitude of the associated time function from above and by the peak amplitude of the corresponding FT from below.

$$X_m^2 T_x^{-1} \leqq E_x \leqq x_m^2 T_x \quad (10a)$$

$$H_m^2 T_h^{-1} \leqq E_h \leqq h_m^2 T_h \quad (10b)$$

$$Y_m^2 T_y^{-1} \leqq E_y \leqq y_m^2 T_y. \quad (10c)$$

These results follow directly from the use of (8).

3.2 Kinetic, potential, and dissipated energies

For a simple oscillator with unit mass, a natural frequency ω_o, and a viscous damping λ, the following relationships exist for the kinetic energy $[T(t) = \dot{y}^2/2 \leftrightarrow T(\omega)]$, the potential energy $[V(t) = \omega_o^2 y^2/2 \leftrightarrow V(\omega)]$, and the dissipated energy $[D(t) = \lambda\omega_o^2 y\dot{y} \leftrightarrow D(\omega)]$,

of the system

$$T(\omega) = \frac{1}{4\pi}[\dot{Y}(i\omega)*\dot{Y}(i\omega)] \tag{11a}$$

$$V(\omega) = \frac{\omega_o^2}{4\pi}[Y(i\omega)*Y(i\omega)] \tag{11b}$$

$$D(\omega) = \frac{\lambda\omega_o^2}{2\pi}[\dot{Y}(i\omega)*Y(i\omega)], \tag{11c}$$

where $\dot{y}(t) \leftrightarrow \dot{Y}(i\omega) = (i\omega)Y(i\omega)$. The proof of these equations is obvious. Using the relationship $Y(i\omega) = H(i\omega)X(i\omega)$ with a simple FT routine, (11a) through (11c) allow various energy functions of time to derive directly from $X(i\omega)$ and $H(i\omega)$.

3.3 Maximum response bounds

Various upper and lower bounds of the maximum temporal response $y_m = \max |y(t)|$ can also be established. Let l_i denote lower bounds and u_i denote upper bounds of $y_m (i = 1, 2, \cdots)$, then the following relation holds:

$$l_2 \leqq l_1 \leqq y_m \leqq \begin{cases} u_1 \\ u_2 \\ u_3 \\ u_4 \end{cases} \leqq \begin{cases} u_5 \leqq u_8 \\ u_6 \\ u_7 \end{cases}, \tag{12}$$

where

$$l_1 = \max_t [E_y(t)/t]^{\frac{1}{2}}, \qquad l_2 = Y_m/T_y, \qquad u_1 = (E_y\Omega_Y/\pi)^{\frac{1}{2}},$$

$$u_2 = (E_xE_h)^{\frac{1}{2}}, \qquad u_3 = S_{y,n}/(t_y)^n, \qquad u_4 = \left| \begin{matrix} \Omega_Y \\ V \quad Y(i\omega) \\ -\Omega_Y \end{matrix} \right| / |2\pi t_y|,$$

$$u_5 = \Omega_Y Y_m/\pi, \qquad u_6 = (\Omega_Y E_x/\pi)^{\frac{1}{2}} H_m, \qquad u_7 = (\Omega_Y E_h/\pi)^{\frac{1}{2}} X_m,$$

and

$$u_8 = \Omega_Y X_m H_m/\pi.$$

The symbol V in the expression of u_4 indicates the total variation.

The lower bounds shall be proved first. Considering the running FT of $y(t)$ according to (1b) and applying Schwartz inequality, the following can be written

$$\begin{aligned} |Y(t, i\omega)|^2 &\leqq \int_0^t |y(\tau)|^2 d\tau \int_0^t |\exp(-i\omega\tau)|^2 d\tau \\ &\leqq E_y(t)t \\ &\leqq [\max_{0 \leqq \tau \leqq t} |y(\tau)|]^2 t^2. \end{aligned} \tag{13}$$

Therefore, for all ω and t,

$$\max_{0 \leqq \tau \leqq t} |y(\tau)| \geqq \left(\frac{E_y(t)}{t} \right)^{\frac{1}{2}} \geqq \frac{|Y(t, i\omega)|}{t} \tag{14a}$$

and

$$y_m \geqq \max_t \left[\frac{E_y(t)}{t} \right]^{\frac{1}{2}} \geqq \frac{Y_m}{T_y}, \tag{14b}$$

which gives the lower bounds l_1 and l_2. Note that $(E_y/T_y)^{\frac{1}{2}}$ and $[E_y(t_y)/t_y]^{\frac{1}{2}}$ are two special cases of l_1, and that l_1 occurs at large (or small) t if the energy function $E_y(t)$ increases faster (or slower) than t. For a given structure, Y_m is fixed; therefore, the bound l_2 decreases with T_y. Note also that, in (14a), the quantity $\max_{t,\omega} [|Y(t, i\omega)|/t]$ should be the exact expression for l_2. However, the current expression Y_m/T_y is more convenient to use than the exact expression that requires the computation of the running spectrum over the entire $t - \omega$ plane. Clearly, better lower bounds for the maximum response can be established on the knowledge of the total energy of the response than on the knowledge of the peak Fourier spectrum of the response.

It is interesting to compare the lower bounds in (12) with the bound Liu[10] establishes for a specific case. For a simple linear oscillator with natural frequency ω_o and viscous damping λ, it has been shown that the maximum displacement response

$$y_m \geqq \frac{1}{p} |X(i\omega)|_{\omega=p} = l_3, \tag{15}$$

where $p = (1 - \lambda^2)^{\frac{1}{2}}\omega_o$. In this situation, the corresponding $H(i\omega) = (-\omega^2 + 2i\omega\omega_o + \omega_o^2)^{-1}$ and $H_m = (2\lambda\omega_o p)^{-1}$ occurring at $\omega = \omega_H = (1 - 2\lambda^2)^{\frac{1}{2}}\omega_o$. Therefore, the bound l_2 gives $y_m \geqq |X(i\omega)|_{\omega=\omega_H}/(2p\omega_o T)$, and in (15) l_3 gives $y_m \geqq |X(i\omega)|_{\omega=p}/(p)$. Clearly, if damping is small, i.e., if $\omega_H \approx p$, then $l_2 < l_3$ when $2\lambda\omega_o T > 1$, $l_2 > l_3$ when $2\lambda\omega_o T < 1$, and $l_2 = l_3$ when $2\lambda\omega_o T = 1$.

The upper bounds, u_1 through u_8, will now be derived. The bound u_1 follows from the use of (4a) and the assumption $t_y \leqq T_y$; u_2 is obtained from applying Schwartz inequality to the relation $y(t) = x(t)*h(t)$; u_3 is obtained directly from (4c); u_4 is a special case of u_3 when $n = 1$ (Giardina[11] proves this differently); u_5 and u_8 follow from u_1 and the relation

$$E_y = \frac{1}{2\pi} \int_{-\Omega_Y}^{\Omega_Y} |Y(i\omega)|^2 d\omega \leqq \frac{\Omega_Y}{\pi} Y_m^2 \leqq \frac{\Omega_Y}{\pi} X_m^2 H_m^2; \tag{16}$$

and u_6 and u_7 follow from u_1 and the relation

$$E_y = \frac{1}{2\pi} \int_{-\Omega_Y}^{\Omega_Y} |X(i\omega)H(i\omega)|^2 d\omega \leqq H_m^2 E_x \quad \text{or} \quad X_m^2 E_h. \tag{17}$$

Generally, better bounds can be obtained when more is known about the input, the transfer characteristics, and the output. For example, the poorest bound in (12) is obviously u_8 because the band-limit Ω_Y and the peak values of spectra $|X(i\omega)|$ and $|H(i\omega)|$ are all that are known. Closer bounds can be established if Ω_Y and Y_m are known, or, equivalently, E_x and H_m, or E_h and X_m. Still closer bounds can be obtained if the energy functions E_y or E_x and E_h are known. Knowledge of E_y, in most cases, depends on the knowledge of $y(t)$ or $Y(i\omega)$; the exact value of y_m can be readily obtained from this knowledge. Therefore, bounds depending on E_y explicitly, such as l_1 and u_1, may not help in practical applications. Note that bounds u_1, u_2, and u_6 grow with T_y; therefore, they do not provide good results for large T_y, i.e., when long excitations or small damping sustain the response for some time. The bound u_2 depends only on the knowledge of the input and the transfer function; therefore, it is convenient to use. Furthermore, it is independent of the output information, thus, it cannot be considered one of the better bounds, especially for very small or very large time t. Bounds u_6, u_7, and u_8 also depend mainly on the input and the transfer function, and the only output knowledge required is the band-limit frequency Ω_Y. Bounds u_3 and u_4 are generally better, yet they require the prior knowledge of t_y, the time when the maximum response occurs. This is usually difficult to know without the waveform or FT of the response. Additional calculations are also needed for the following two bounds: for u_3, the calculation of $S_{y,n}$ and the areas under the spectra of $Y(i\omega)$ and its derivatives, and for u_4, the absolute value of the total variation of the complex quantity $Y(i\omega)$ for the entire frequency axis. For u_3, small n provides better bounds for small t, and large n for large t. For u_4, it provides better bounds for large t than for small t. In general, u_1, u_3, and u_4 are better upper bounds, yet they are less convenient to use than others.

Some interesting features about these response bounds are noteworthy. Drenick[12] derives the least favorable excitation for structures based on u_2. An uncertainty condition $T_y\Omega_Y \geqq \pi$, familiar in band-limited and time-limited signal analysis can be arrived at from bounds l_2 and u_5. The bound u_4 can be used to estimate the settling time t_ϵ for the response $y(t)$ to remain with a specified value ϵ[10]. For example, if $Y_1(i\omega)$ is smoother, and thus has less variation than $Y_2(i\omega)$, then $y_1(t)$ takes longer than $y_2(t)$ to settle to the level ϵ. This implies that, for two comparable response Fourier spectra, the smoother one corresponds to the response of a system with higher damping and the rugged one corresponds to the response with less damping.

3.4 Mean square response

If $x(t)$ and hence $y(t)$ are random, the mean square response $\sigma_y^2 = E[|y(t)|^2]$ (where E denotes expectation) is of interest. Let $\sigma_x^2 = E[|x(t)|^2]$, and $S_x(i\omega)$ and $S_y(i\omega)$ be the power spectral density functions, and $R_x(\tau)$ and $R_y(\tau)$ be the autocorrelation functions of $x(t)$ and $y(t)$, respectively, then the following relations regarding σ_y can be found:

$$\sigma_y^2 = R_y(0) = \int_0^\infty R_h(\tau) R_x(\tau) d\tau \tag{18a}$$

$$\sigma_y^2 = \frac{E[E_y]}{T_y} = \frac{E[|X(i\omega)|^2]}{2\pi T_y} E_h \tag{18b}$$

$$\sigma_y^2 \leqq \frac{\sigma_x^2}{2\pi} H_m^2. \tag{18c}$$

In (18a), $R_y(\tau) = R_h(t) * R_x(t)$, $R_h(\tau) = \int_0^{T_h} h(t) h(t - \tau) dt$ = the system autocorrelation function, as defined in (1k). Because the proofs of these equations are straightforward, they are omitted. The mean square response can be provided either by (18a) upon a simple time integration of the product of the autocorrelation functions of input and impulse response, or by (18b) upon the direct knowledge of the mean output energy or the expected square input Fourier spectrum. Equation (18c) provides a simple upper bound based on mean square value of input and the peak amplitude of the frequency response of the system.

3.5 Relations regarding input and output time histories

The following useful equations relate the time histories of input and output:

$$\begin{Bmatrix} x(t) \\ y(t) \end{Bmatrix} = \exp(i\omega t) \begin{Bmatrix} \partial X(t, i\omega)/\partial t \\ \partial Y(t, i\omega)/\partial t \end{Bmatrix}$$

$$= \exp(-i\omega t) \begin{Bmatrix} \partial X^c(t, i\omega)/\partial t \\ \partial Y^c(t, i\omega)/\partial t \end{Bmatrix} \tag{19}$$

$$x(t) y(t) = \frac{1}{2\pi} \int_0^\infty \mathrm{Re}\,[H(i\omega)] \rho_x(t, i\omega) d\omega \tag{20}$$

$$y(t) = \sum_{j=0}^{n} \frac{m_j x^{(j)}(t)}{j!} \tag{21}$$

$$x(t) = \frac{1}{m_0} \sum_{j=0}^{n} \frac{n_j y^{(i)}(t)}{j!}, \tag{22}$$

where

$$m_j = \int_{-\infty}^{\infty} t^j h(t)dt, \qquad n_0 = (m_1/m_0), \qquad n_1 = (m_1^2/m_0 - m_2/2),$$

$$n_2 = [m_1^3/m_0 - (1 + m_0)m_1m_2/2m_0 - m_3/6m_0], \cdots, \quad \text{etc.},$$

and the superscript c in (19) indicates the complex conjugate.

Equation (19) expresses the waveform of input or output in terms of the corresponding running spectrum and can be used to recover it; (20) gives the instantaneous value of the multiple of $x(t)$ and $y(t)$ as a simple frequency integral in terms of the transfer function and instantaneous power spectrum density of the input; (21) [or (22)] expresses the output (or the input) waveform in terms of the moments of the impulse response function of the system and the derivatives of the input (or the output). Liu[13] derives (19) and (20). Papoulis[14] uses Taylor's expansion to derive (21) and (22). Note that (21) and (22) are useful only if the two series converge rapidly; i.e., if the transfer function $H(i\omega)$ only takes significant values and can be approximated by a polynomial of low order within the region of $|\omega| \leqq \Omega_Y$.

IV. SHOCK AND VIBRATION ANALYSIS OF SIMPLE STRUCTURAL SYSTEMS

The relations presented above can be applied in the shock and vibration analysis of structures. Since many structures can be treated as systems with a single mode of oscillation and many others can be solved by superposition of various modal responses in the generalized coordinates, the application can be well illustrated by the analysis of simple structures. We therefore consider a set of single-degree-of-freedom systems with natural frequency in the range of 0.05 to 10 Hz (most commercial and industrial structures have natural frequency in this range), and having a damping ratio of $\lambda = 2$ percent and 10 percent, respectively. These structures are subjected to a random transient load resembling a strong-motion earthquake accelerogram (Fig. 1) and four different types of idealized impulses resembling air or ground shocks (Fig. 2). The various bounds of the relative displacement and acceleration responses of the structures are calculated according to (12) and compared with the actual maximum response y_m. The results in Fig. 3 indicate that, for earthquake type of excitations, the lower bound l_1 and the upper bound u_3 (with $n = 0$) are the better bounds; u_4 and u_1 also appear as reasonably good upper bounds although, for the acceleration response, they show wider fluctuations than u_3. Bounds l_2 and u_5 fluctuate with Y_m and vary with the natural

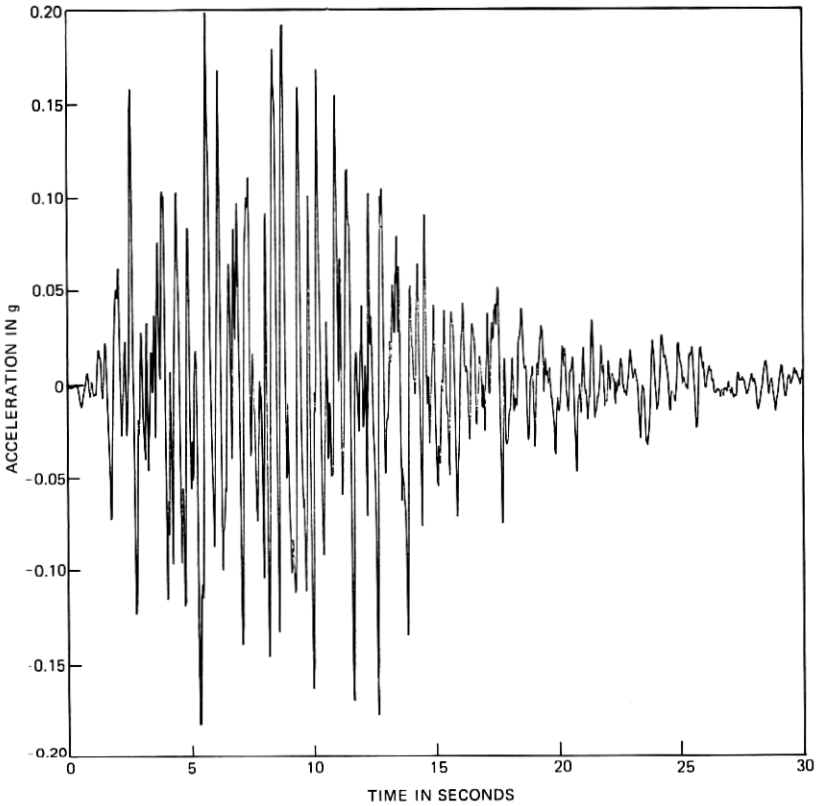

Fig. 1—A random transient waveform.

frequency of the structure, ω_o; therefore, both have the same degree of closeness to the real response. Bounds u_6, u_8, and l_2 provide rough estimates of the response; this is expected because little information is needed about the input, the output, or the structure. Bounds u_6 and u_8 are constant for the acceleration response (see Figs. 3a and 3b) because, for a fixed input, E_x and X_m are both constant, and the simple structures considered, $H_m = (2\lambda)^{-1}(1 - \lambda^2)^{-\frac{1}{2}}$, i.e., the maximum spectrum of the transfer function associated with the relative acceleration response is a constant for a given damping, and is independent of ω_o. Bounds u_6 and u_8, for the displacement response, decrease with ω_o (see Figs. 3c and 3d) because the associated $H_m = (2\lambda p)^{-1}$. Bounds u_2 and u_7, for the acceleration response, grow with $E_h^{\frac{1}{2}}$, which increases with ω_o. For the displacement response, u_2 appears also to be a reasonably good bound.

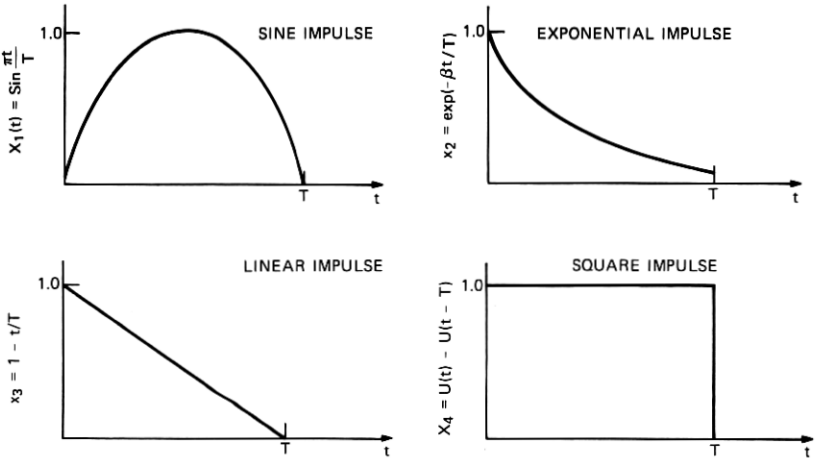

Fig. 2—Impulse loads.

The results for various types of impulse loads are generally similar and can be represented by Fig. 4. For impulsive types of excitations, we can make the following general observations: (*i*) l_1 seems to be a very good bound for most cases ($l_1 \approx y_m$ when $\omega \to 0$ or when ω is small), (*ii*) the best upper bound is u_3 ($n = 0$), which is very close to y_m, particularly for the displacement response, (*iii*) u_6 and u_8, because they are constant for the acceleration response and decrease with ω_o for displacement response, do not appear to be good upper bounds, (*iv*) for the acceleration response, u_2 and u_7 increase with ω_o; the rate of increase is reduced in high-damping cases, (*v*) for the displacement response, $u_5 \to u_8$ and $u_7 \to u_1$, when $\omega \to 0$, and (*vi*) next to u_3, u_2 and u_4 seem adequate as upper bounds.

V. APPLICATIONS TO TELEPHONE STRUCTURES IN AN EARTHQUAKE AREA

The above analysis can be applied to shock and vibration problems of telephone structures. Examples are the dynamic response analysis and aseismic design of various telephone building and equipment systems located in an earthquake area. Some of such applications will be described below.

5.1 Aseismic design of battery stands

It has been recognized[15] that, in large areas of the country susceptible to earthquakes, battery stands on floors of multistory telephone build-

ings require special physical design consideration to protect the safety of operating personnel and the reliability of telephone plant. Figure 5 shows a typical soft-site stand modified for service in earthquake areas. It consists of bracing to support the stand laterally from an overhead ironwork structure and to support the cells on the shelves. Clearance is provided around the entire cell to allow it to rattle around freely in response to ground motion. The failure of the battery stand generally occurs from excessive acceleration, which could lead to sliding and rattling of cells and their banging against one another and against the side racks, and from excessive displacement of the stand that could result in overstress of the column members of the stand. Therefore, the displacement and acceleration responses of the stand are of crucial concern to its aseismic adequacy. These response parameters can be estimated very conveniently by the response-bound relations derived in Section III. We assume that all that is known about the physical property of the battery stand is that it has a damping ratio about 2 percent and a natural frequency in the range of 3 to 5 Hz.[16] It is reasonable to assume that the floor motion corresponding to a large earthquake resembles the waveform shown in Fig. 1. The peak acceleration amplitude would be in the range of 0.75 g because of the soil and building amplification of the ground motion. From the analysis in Section IV, the response bounds of the battery stands shown in Fig. 6 can be readily established. From the acceleration lower bound l_1 in Fig. 6 that provides an underestimate of the actual responses, it is immediately clear that the natural frequency of the battery stand in the range of 1.5 to 3 would not be desirable. Because the high acceleration level in this range would cause lateral forces exceeding the friction force between the base of the cells and the supporting shelves, the battery would then slide and rattle violently in response to ground motion. The displacement bounds u_3 and l_1 indicate a continuously decreasing trend with the natural frequency of the stand. The upper bound u_3, which provides a conservative estimate, indicates that, if the battery stand is designed to have a natural frequency higher than 5 Hz, the actual maximum displacement response would be less than the acceptable limit, e.g., about 3 inches. We can therefore conclude from such a simple analysis that, from consideration of both the acceleration and displacement responses, it is desirable to increase the frequency of the battery stand up to about 5 Hz or above. The increase of the frequency or, equivalently, the stiffness of the stand can be generally achieved by adding bracings to the wall, columns, or to superstructures such as the auxiliary frames.

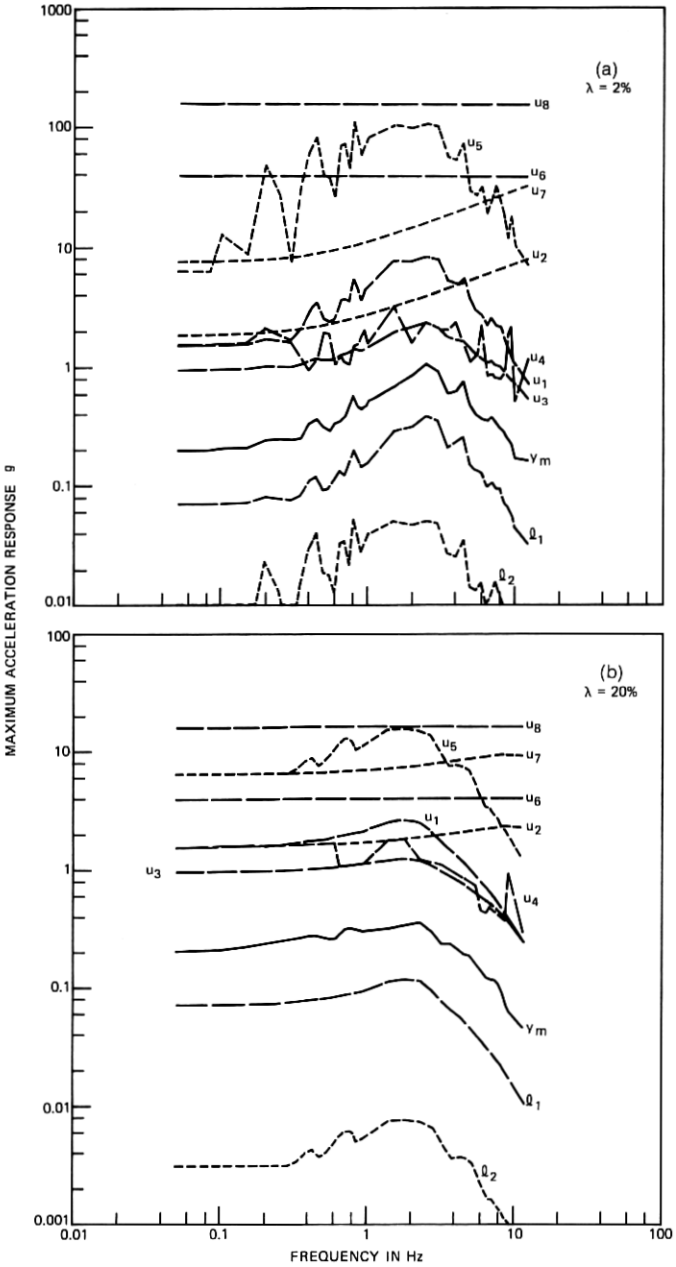

Fig. 3—Response bounds of single-degree-of-freedom structures subjected to random load.

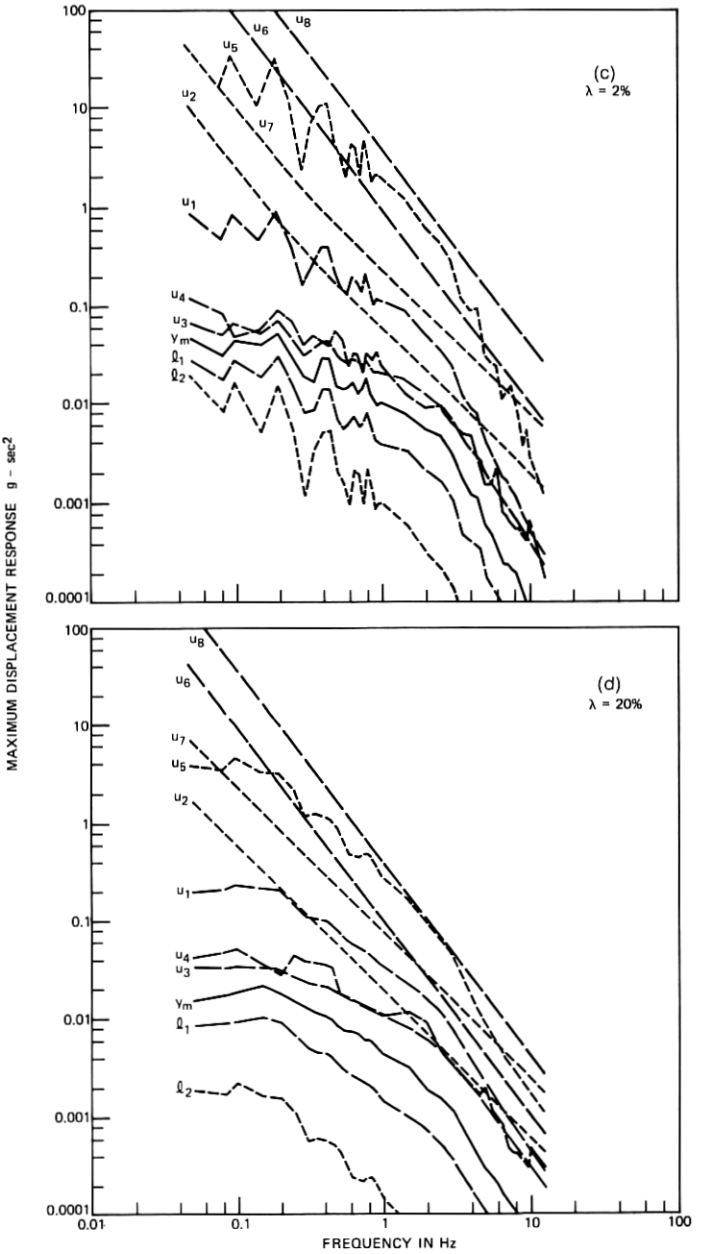

Fig. 3 (continued).

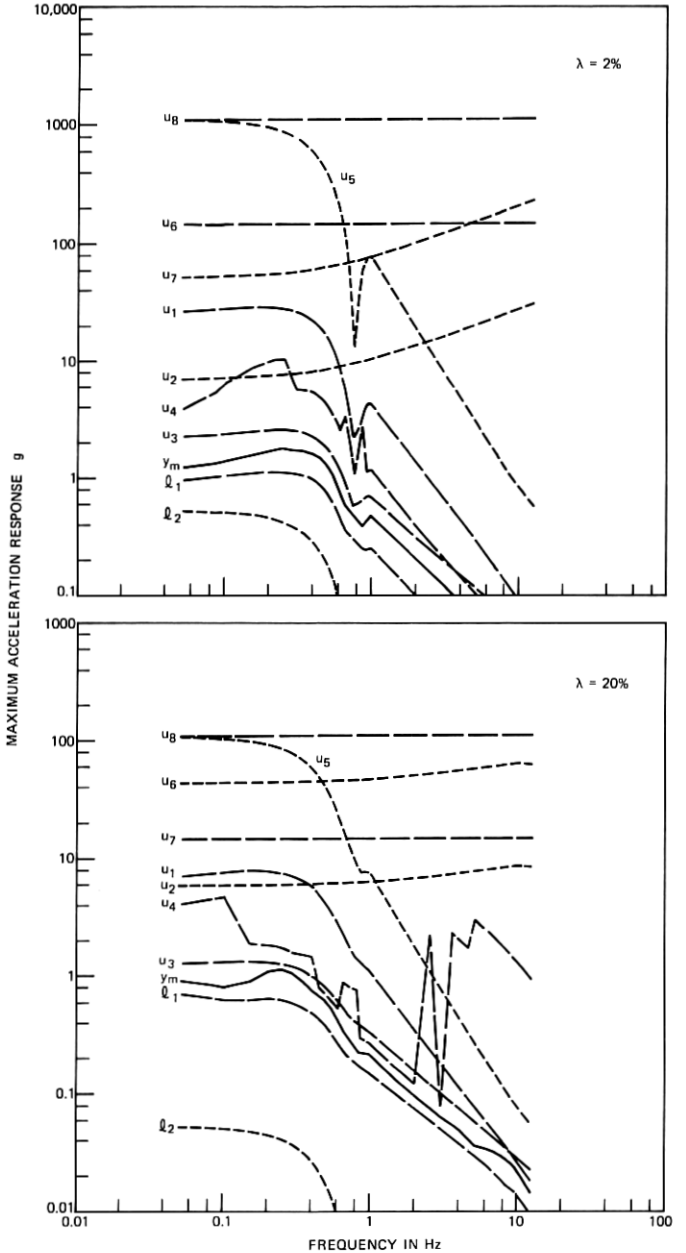

Fig. 4—Response bounds of single-degree-of-freedom structures subjected to sine impulse.

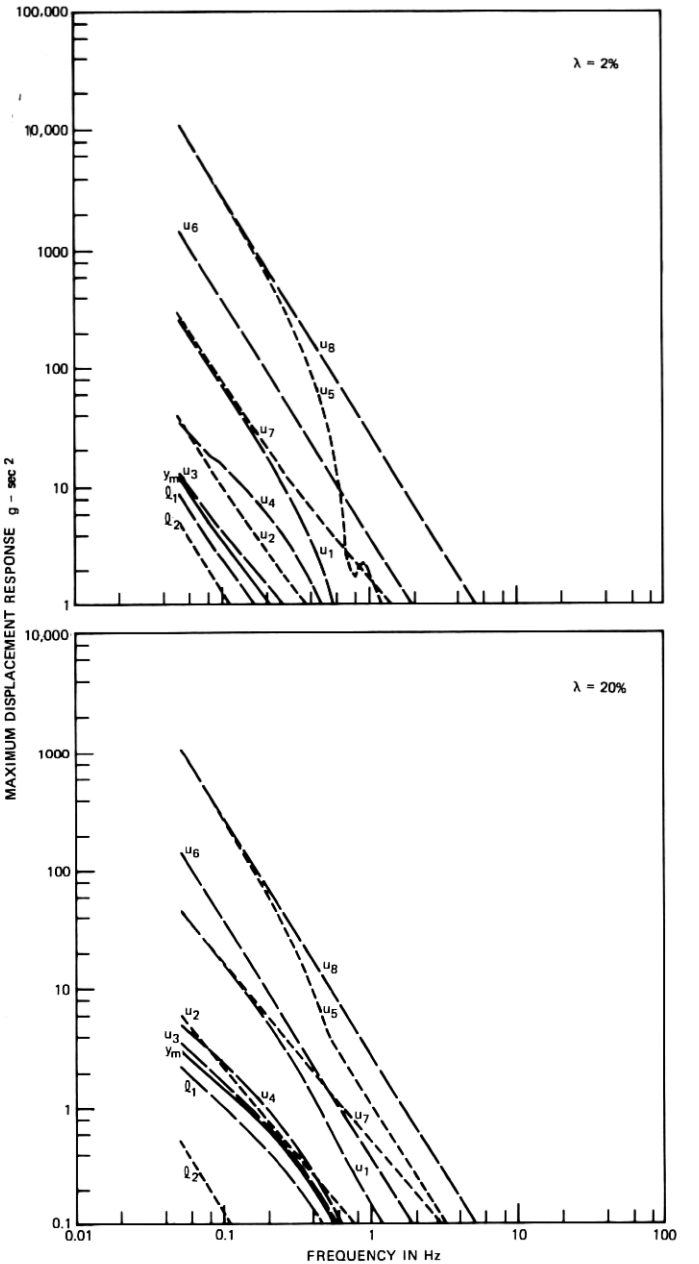

Fig. 4 (continued).

Fig. 5—Soft-site battery stand modified for service in earthquake area.

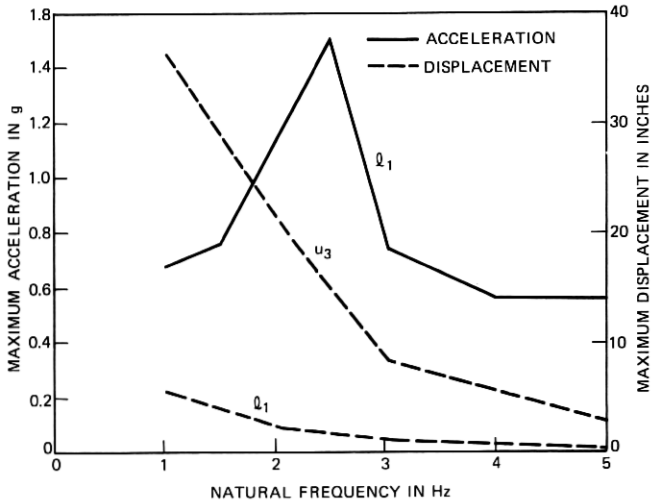

Fig. 6—Response bounds of battery stands.

5.2 Earthquake adequacy of community dial offices

A community dial office (CDO) is a small telephone office housing mostly step-by-step equipment servicing a local community. The CDO buildings are generally one-story concrete block constructions, with a few steel-frame constructions as exceptions.

Tests and analyses relating to typical CDO facilities[17,18] have indicated seismic weaknesses in the equipment connective system, particularly at the junction of the superstructure bracing system to the building. Figure 7 shows a schematic cross-sectional representation of a typical CDO equipment support structure. Equipment frame lineups are generally tied together at the 9-foot level by cross-aisle cable racks and angle braces (indicated as lineup braces). On the common distribution frame (CDF) side, the frames are attached to a wood batten on the building wall by horizontally oriented cable racks and angle braces (indicated as wall braces).

While there are several possible failure modes of CDO equipment, the most likely and the most critical one is the failure of the lateral

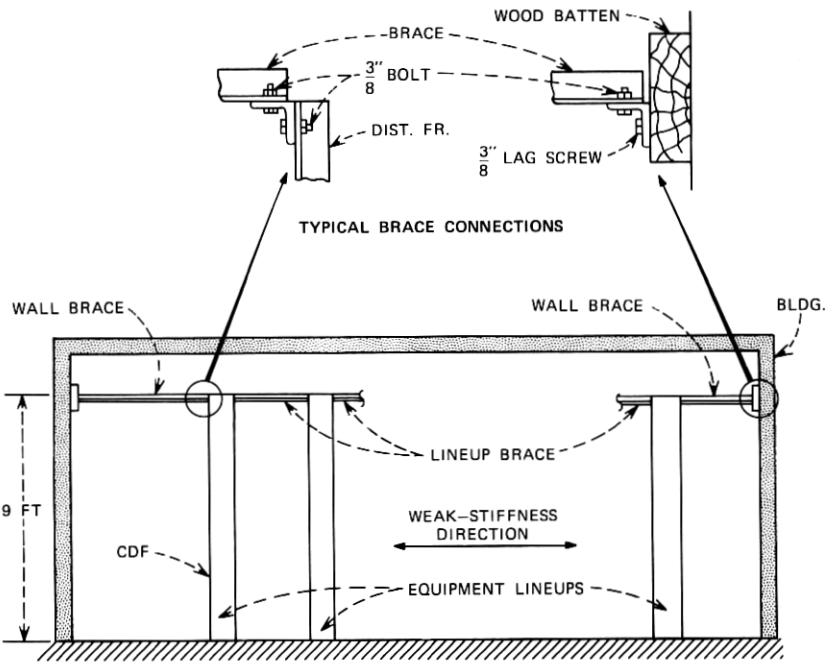

Fig. 7—Typical CDO support system.

support system during severe ground shaking. The wood batten shown in Fig. 7 is attached to the building wall by either lag screws into wood studs, lag into lead expansion shields inserted into concrete blocks, or toggle bolts into concrete blocks, depending on the building construction. This batten could pull away from the wall and result in the collapse of the equipment. To determine whether such a failure might occur, it is necessary to compare the axial force of the wall bracing development during the earthquake with the allowable force. The wall force is given as $F = EA\delta/l$, where E is the modulus of elasticity, A and L are the cross-sectional area and length of the wall brace, respectively, and δ is the relative displacement between the two ends of the wall brace. From testing or analysis we assume the transfer function $H_\delta(\omega)$ for the relative displacement response δ of a hypothetical CDO system as given in Fig. 8. We wish to find the earthquake-resistant capacity of this system, e.g., the highest ground acceleration this system can safely withstand.

A typical wall brace is made of steel with $E = 30 \times 10^6$ pounds per square inch, $A = 0.53$ square inch, and $L = 5.7$ inches. By testing we found that the maximum axial force the wall brace can take without pulling out of lag screws or toggle bolts is 900 pounds, which corresponds to a maximum lateral relative displacement of $\delta = 0.003$ inch between the two ends of wall brace. Based on the transfer function, $H_\delta(\omega)$, and the results described in Section IV, we found that a conservative estimate (u_3) of the maximum displacement corresponding

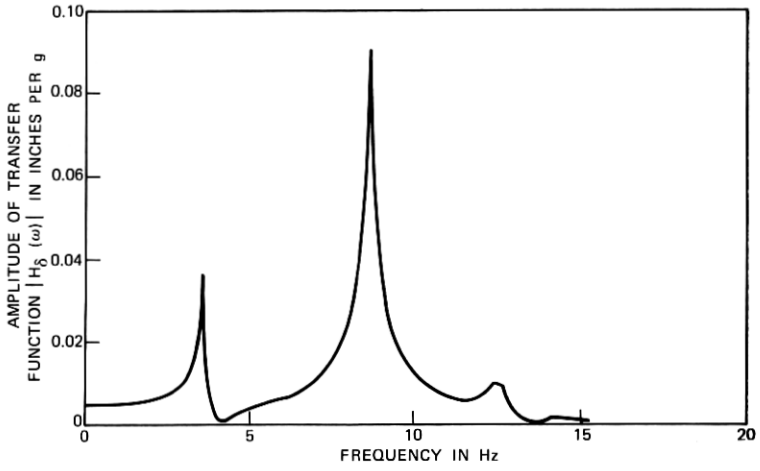

Fig. 8—Transfer function of CDO system.

to a 0.2 g earthquake loading is approximately 0.002 inch. Assuming the system remains linearly independent of the input amplitude, we can conclude that the hypothetical CDO system under consideration is capable of resisting earthquake ground acceleration up to about 0.3 g, a motion equivalent in magnitude to the El Centro 1940 earthquake. Additional braces would be needed if higher acceleration level is expected at the site.

VI. CONCLUSION

Various equality and inequality input-transfer-output relations are derived to facilitate the application of the Fourier transform method in the shock and vibration analysis of linear structural systems. In particular, a set of lower and upper bounds of the maximum response is obtained. Such bounds allow various maximum response parameters to be easily estimated with little computation effort. The accuracy of the estimate depends on the degree of availability of information about the input, the transfer function, and the response of the system. In general, l_1 and u_3 appear to be reasonably good lower and upper estimates of the maximum response, respectively. Estimates of response bounds of simple systems are examined when subjected to a random transient excitation and impulse loadings. For systems whose transform functions roll off quickly at high frequencies, or for inputs that have fast-decaying Fourier spectra, the relations presented apply reasonably well. Care should be taken with short-duration impulses that have wide spectra. Telephone structures subjected to earthquake excitations, e.g., a conventional battery stand and a CDO system, are considered to demonstrate the practical applications.

VII. ACKNOWLEDGMENTS

The author wishes to thank F. X. Prendergast for careful review of the manuscript, N. J. DeCapua for providing information used in Section V, and M. Dougherty for performing most of the numerical analysis of this paper.

REFERENCES

1. I. N. Sneddon, *Fourier Transforms*, New York: McGraw-Hill, 1951.
2. C. L. Amba-Rao, "Fourier Transform Methods in Elasticity Problems and an Application," J. Franklin Inst., *287*, No. 3 (March 1969), pp. 241–269.
3. P. H. White, "Application of the Fast Fourier Transform to Linear, Distribution Systems Response Calculations," J. Acoust. Soc. Am., Pt 2, *46*, No. 1 (1969), pp. 273–274.
4. R. C. Le Bail, "Use of Fast Fourier Transforms for Solving Partial Differential Equations in Physics," J. Comput. Physics, *9*, 1972, pp. 440–465.

5. S. C. Liu and L. W. Fagel, "Earthquake Interaction by Fast Fourier Transform," J. EM Div., ASCE, *97*, No. EM4 (August 1971), pp. 1223–1237.
6. L. W. Fagel and S. C. Liu, "Earthquake Interaction for Multistory Buildings," J. EM Div., ASCE, *98*, No. EM4 (August 1972).
7. S. C. Kak, "Causality and Limits on Frequency Functions," Int. J. Electronics, *32*, No. 1 (1971), pp. 41–47.
8. A. Papoulis, "Limits on Bandlimited Signals," Proc. IEEE, *55*, No. 10 (October 1967), pp. 1677–1686.
9. A. Papoulis, "Maximum Response with Input Energy Constraints and the Matched Filter Principle," IEEE Trans. on Circuit Theory, *CT-17*, No. 2 (May 1970), pp. 175–182.
10. S. C. Liu, "An Approach to Time-Varying Spectral Analysis," J. EM Div., ASCE, *98*, No. EM1, Proc. paper 8733 (February 1973), pp. 245–253.
11. C. R. Giardina, "An Upper Bound on the Settling Time," IEEE Trans. on Circuit Theory, *CT-19*, No. 9 (July 1972), pp. 372–373.
12. R. F. Drenick, "Model-Free Design of Aseismic Structures," J. EM Div., ASCE, *96*, No. EM4, Proc. paper 7496 (August 1970), pp. 483–493.
13. S. C. Liu, "Time-Varying Spectra and Linear Transformation," B.S.T.J., *50*, No. 7 (September 1971), pp. 2365–2374.
14. A. Papoulis, "Approximations of Point Spread for Deconvolution," J. Opt. Soc. Am., *62*, No. 1 (January 1972), pp. 77–80.
15. H. J. Luer, "Incorporating the New Battery into the Telephone Plant," B.S.T.J., *49*, No. 7 (September 1970), pp. 1447–1470.
16. N. J. DeCapua and M. G. Hetman, "Earthquake Analysis of Battery Stands," unpublished work.
17. R. M. Riley, private communication to W. H. Turner, 1974.
18. N. J. DeCapua and F. X. Prendergast, unpublished work.